



PEGASUS-III  
Experiment

# Investigating The Role of Impurities in Plasma Startup Via LHI on PEGASUS-III

**C. Rodriguez Sanchez**

S.J. Diem, R.J. Fonck, M.D. Nornberg, G.R. Winz

64<sup>th</sup> Annual Meeting of the APS Division of Plasma Physics, Spokane, WA

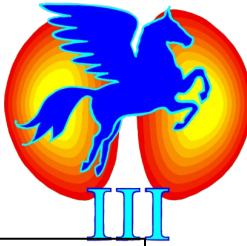
Presentation CP11.00050

17 October 2022

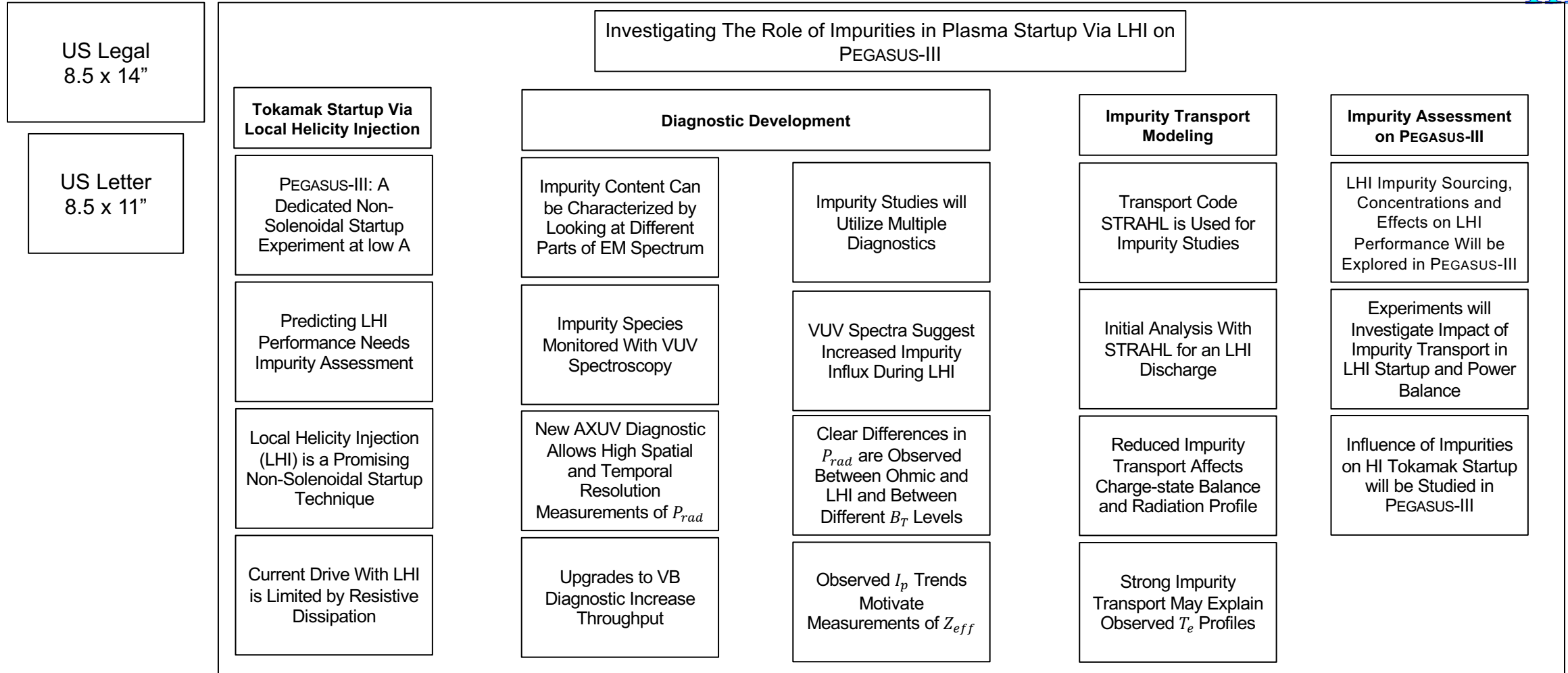


Department of  
Engineering Physics  
UNIVERSITY OF WISCONSIN-MADISON

# Poster Layout



12:1 scale Panel size: 8' x 4'

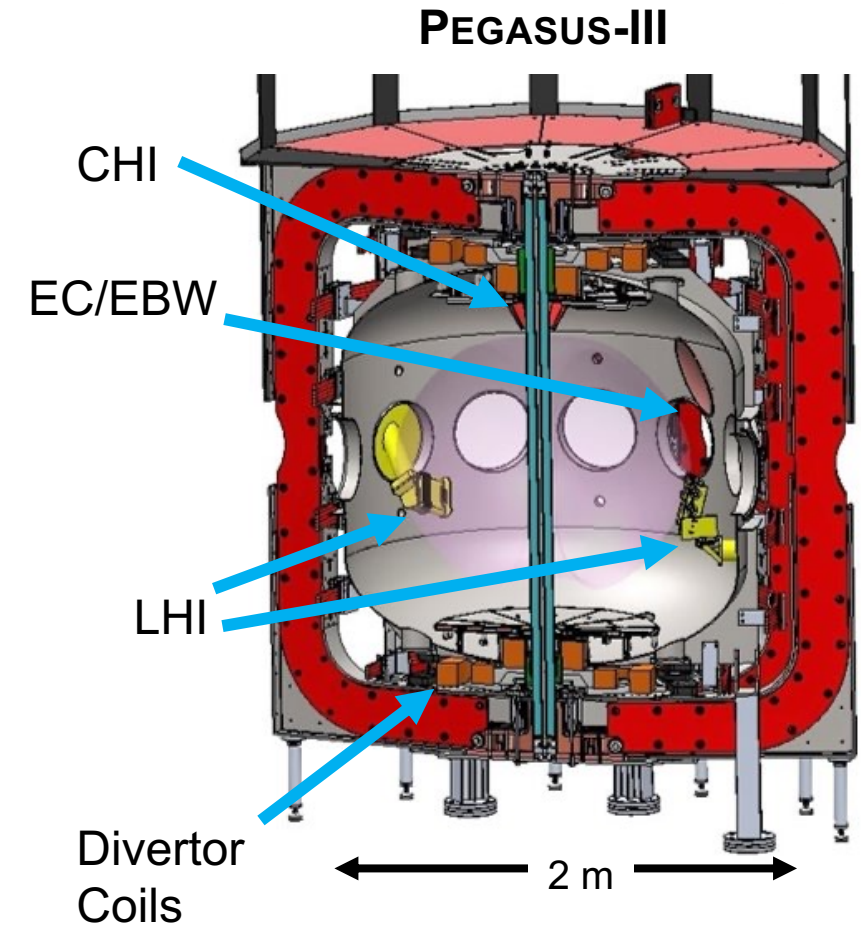


# Tokamak Startup Via Local Helicity Injection

# PEGASUS-III: A Dedicated Non-Solenoidal Startup Experiment at low A



- Future power plants benefit from solenoid-free operations
  - Cost reduction
  - Increased space for shielding and blanket
  - Simplified design
- The new PEGASUS-III facility is a major upgrade to the PEGASUS ST
  - Removal of the Ohmic solenoid
  - Upgraded TF magnet assembly to deliver up to 0.6 T on axis
  - **Mission:** compare, contrast and combine startup techniques
    - Helicity Injection (LHI and CHI)
    - RF heating and current drive (EBW, EC)
- Impurity roles in plasma startup
  - Power balance
  - Limit current drive:  $I_p \sim V/R$



# Predicting LHI Performance Needs Impurity Assessment



- Helicity input balanced by resistive dissipation

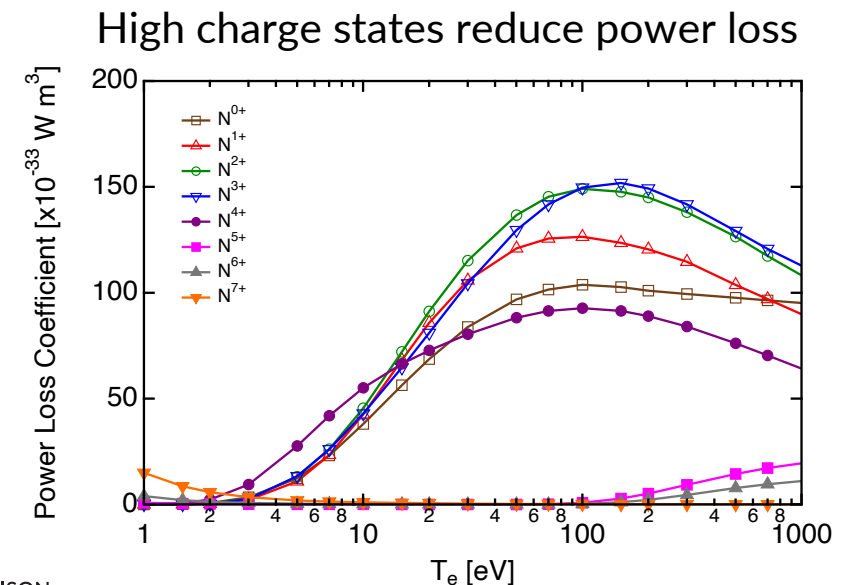
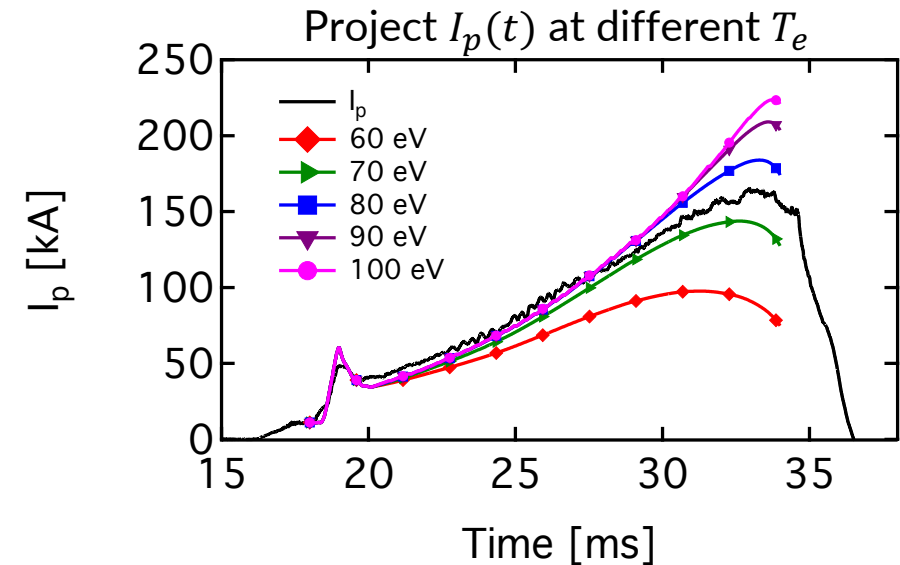
$$\dot{K}_{dis} \approx -\frac{2\pi R_0}{A_p} \langle \eta \rangle I_p \Psi \quad \eta \propto Z_{eff} T_e^{-3/2}$$

- Impurity concentration directly affects resistivity

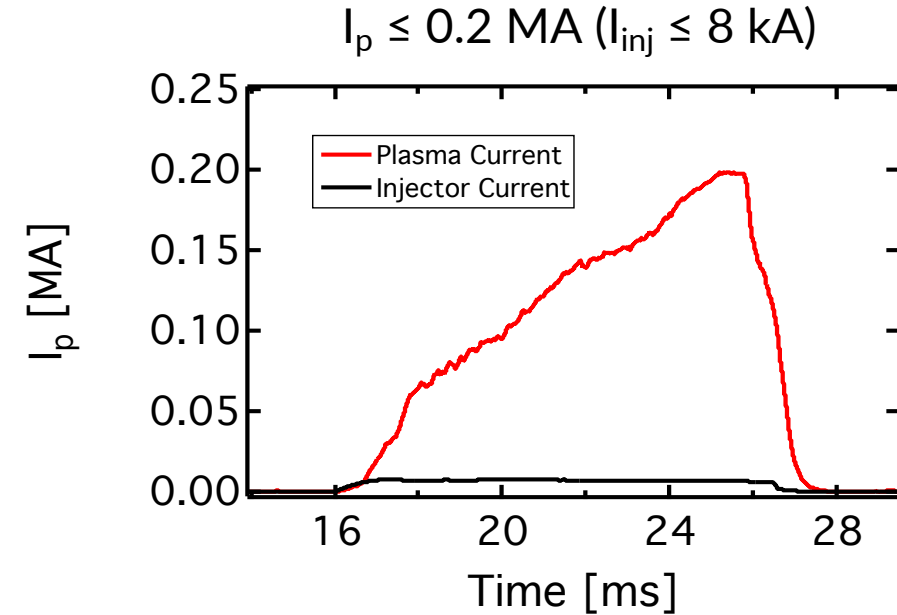
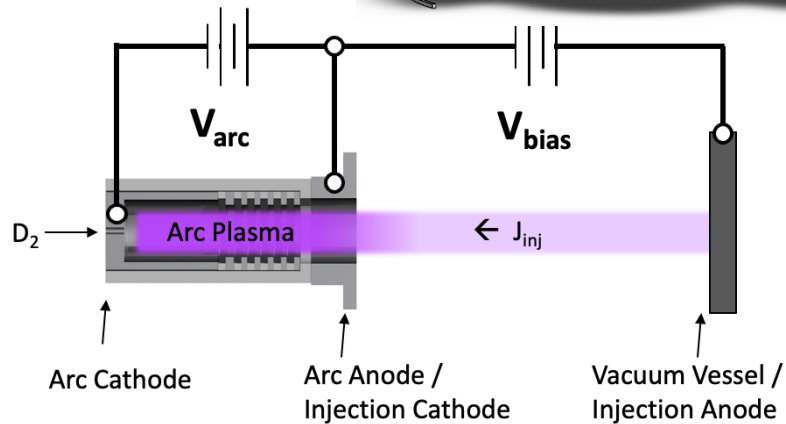
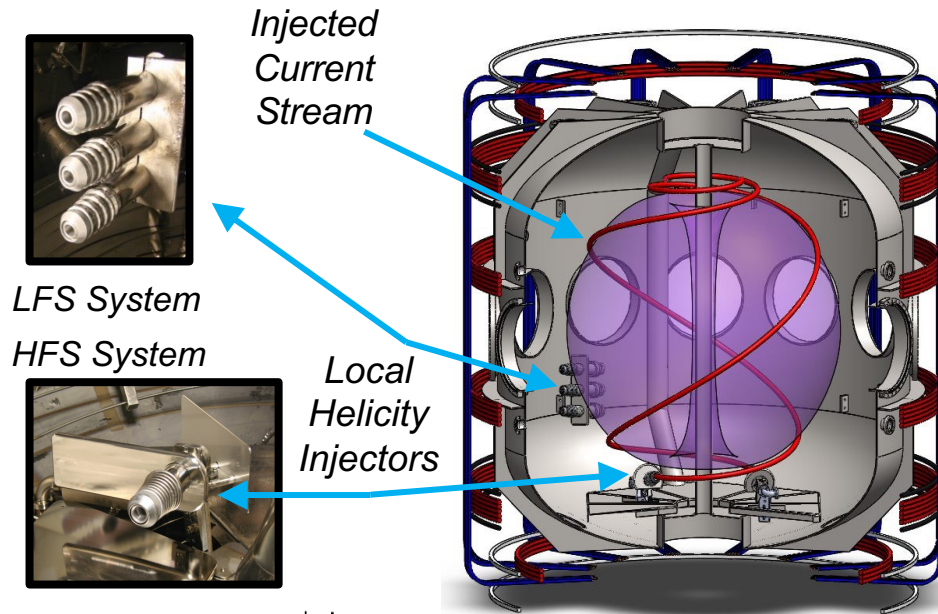
- Increased  $Z_{eff}$
- Plasma cooling

- LHI is useful if its target can couple to other CD

- Acceptably low  $Z_{eff}$
- Power losses do not impact the power balance



# Local Helicity Injection (LHI) is a Promising Non-Solenoidal Startup Technique



- LHI provides solenoid-free startup
  - Edge current extracted from injectors at boundary
  - Relaxation to tokamak-like state via helicity-conserving instabilities
- Used routinely for startup on PEGASUS



# Current Drive With LHI is Limited by Resistive Dissipation



$$K = \int \vec{A} \cdot \vec{B} \, dV \quad \longrightarrow \quad \frac{dK}{dt} = \underbrace{-2 \frac{\partial \psi}{\partial t} \Psi}_{\text{AC Helicity Injection}} - \underbrace{2 \int \phi \vec{B} \cdot \hat{n} \, dS}_{\text{DC Helicity Injection}} - \underbrace{2 \int \eta \vec{J} \cdot \vec{B} \, dV}_{\text{Resistive Helicity Dissipation}}$$

- AC Helicity Injection:

$$\dot{K}_{AC} = -2 \frac{\partial \psi}{\partial t} \Psi = 2V_{\text{loop}} \Psi$$

- DC Helicity injection:

$$\dot{K}_{DC} = -2 \int \phi \vec{B} \cdot \hat{n} \, dS = 2V_{\text{LHI}} \Psi$$

- Resistive Helicity Dissipation:

$$\dot{K}_{dis} = -2 \int \eta \vec{J} \cdot \vec{B} \, dV \approx \frac{2\pi R_0}{A_p} \langle \eta \rangle I_p \Psi$$

- In Steady state, Source = Sink

$$V_{LHI} = V_{inj} \frac{A_{inj} B_{inj}}{\Psi}$$

$$I_p \leq \frac{A_p}{2 \pi R_0 \langle \eta \rangle} (V_{loop} + V_{LHI})$$



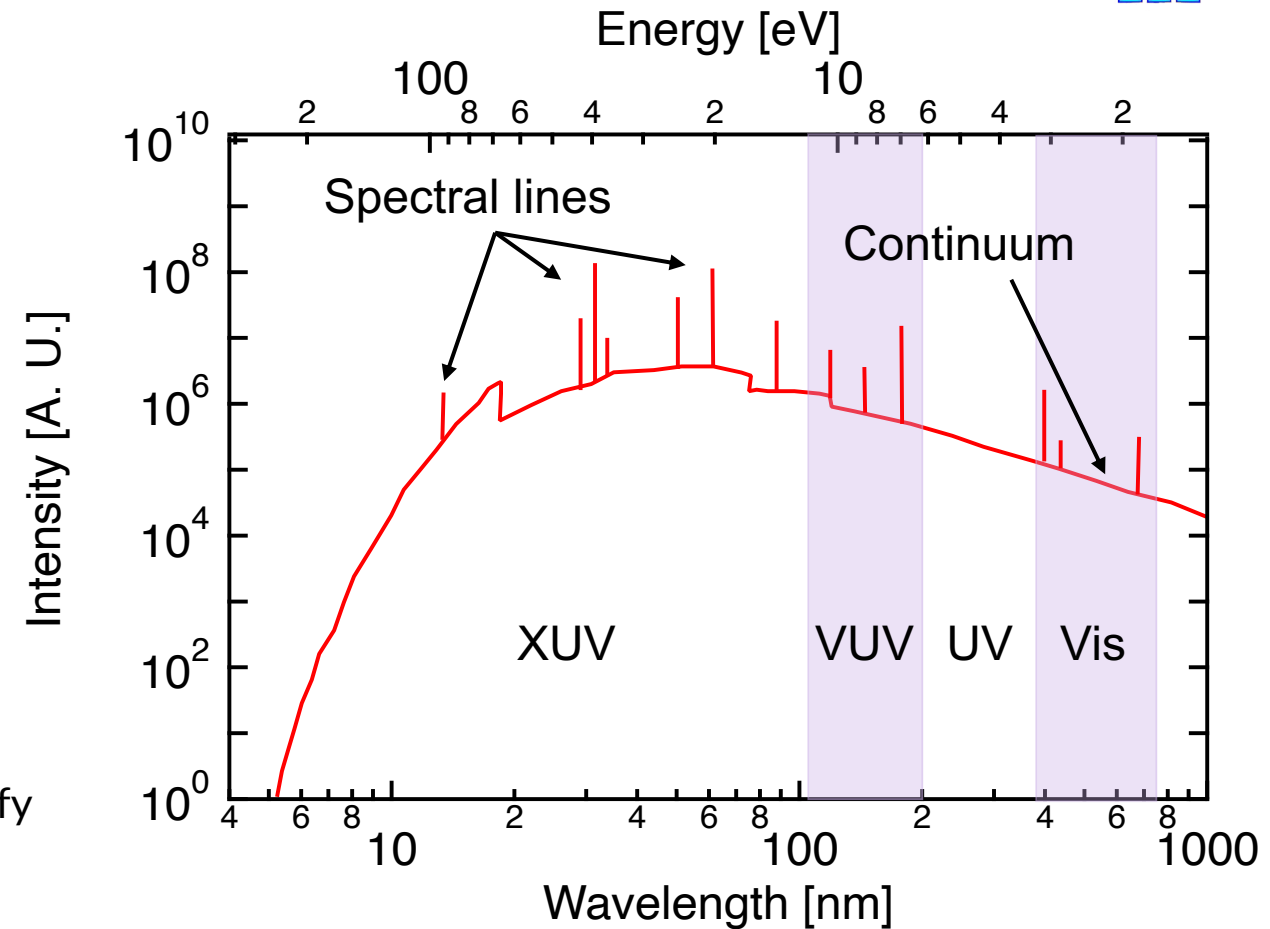
# Diagnostic Development



# Impurity Content Can be Characterized by Looking at Different Parts of EM Spectrum



- Impurities increase EM radiation
  - XUV part contributes the most to power losses
- Bremsstrahlung emission
  - Continuum radiation
  - Electrons slow down after colliding with ions
  - Proportional to ion charge
- Line emission
  - Line emitted from transitions in electrons
  - Bright, resonant lines in the VUV are easy to identify



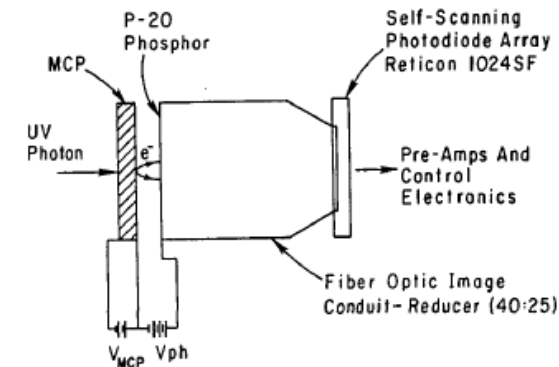
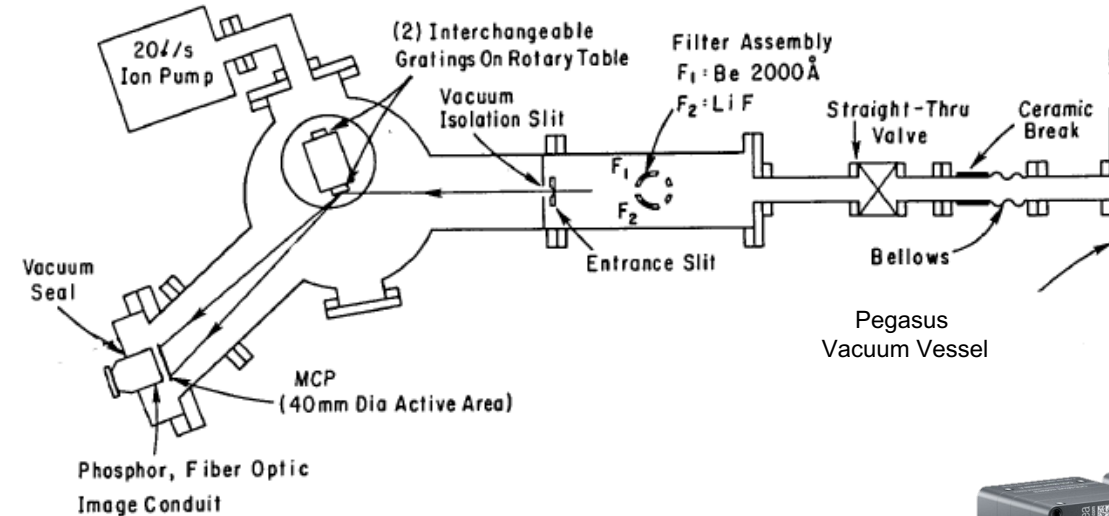
Inspired by: H.-J. Kunze, *Introduction to Plasma Spectroscopy*  
(Springer Berlin Heidelberg, Berlin, Heidelberg, 2009).





# Impurity Species Monitored With VUV Spectroscopy

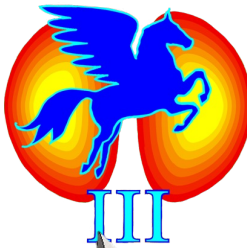
- SPRED VUV Spectrometer
  - Single line of sight at  $R_{\text{tan}} = 20$  cm
- Two interchangeable gratings
  - High resolution grating
    - Spectral Range 10 to 32 nm, resolution 0.04 nm
    - Useful for metallic lines like Mo, W and Ti
  - Low resolution grating
    - Spectral range 15.5 to 170 nm, resolution 0.3 nm
    - Coverage for Li-like to B-like low-z impurity lines
- CMOS image sensor
  - 2048 x 1088 Resolution
  - Temporal resolution  $\sim 1.5$  kHz at 2048 x 120



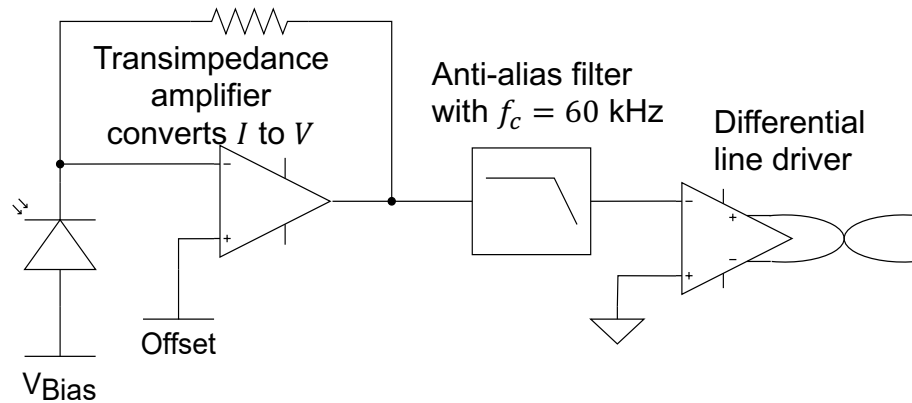
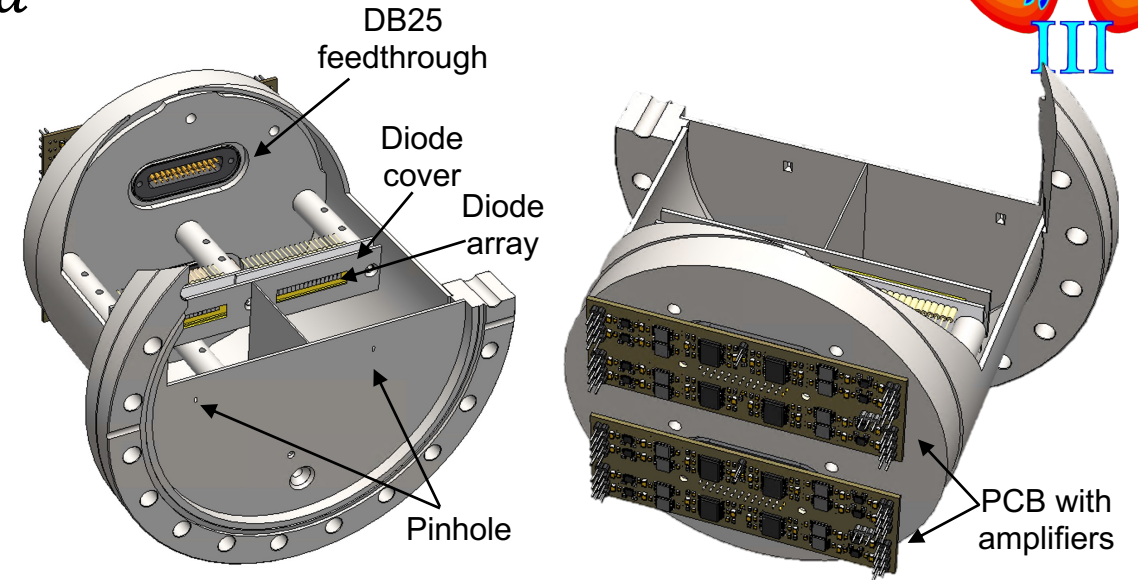
VUV to Visible imaging System



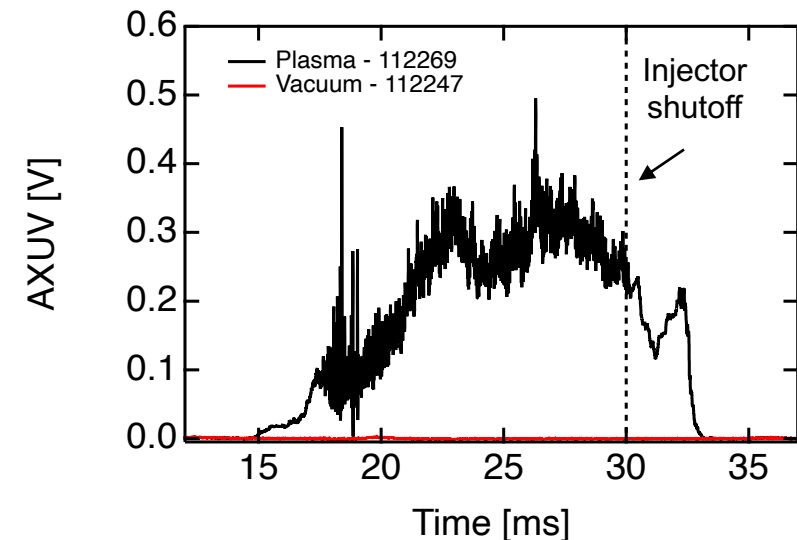
# New AXUV Diagnostic Allows High Spatial and Temporal Resolution Measurements of $P_{rad}$



- Two 16-channel AXUV16ELG photodiode arrays
  - 32 lines of sight
  - $R_{tan} \approx 9 - 90$  cm,  $\sim 2.5$  cm spatial resolution
  - Onion inversion algorithm<sup>1</sup> to obtain  $P_{rad}(R)$
- Three-stage amplifiers for high signal-to-noise ratio



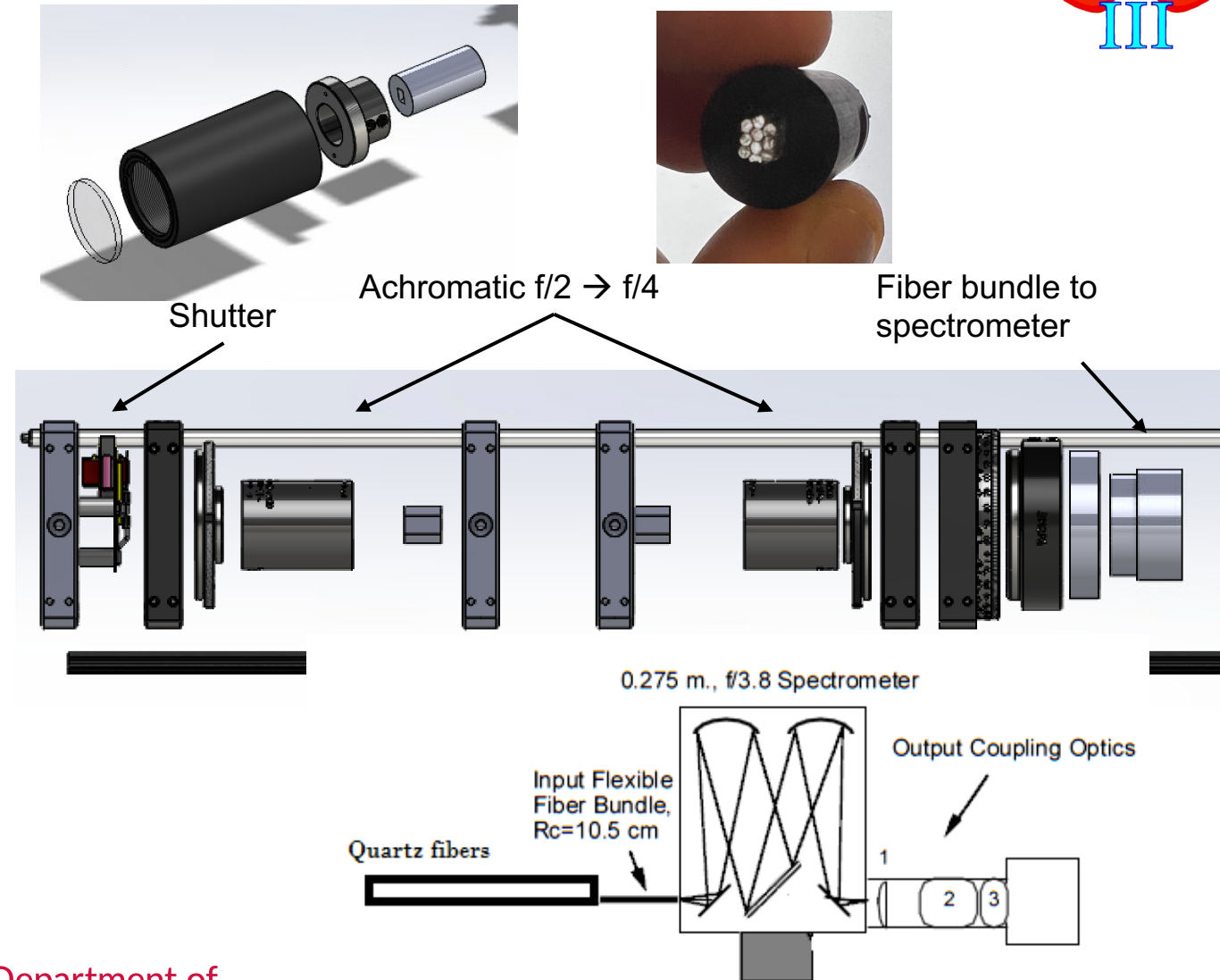
<sup>1</sup> C.J. Dasch, Applied Optics **31**, 1146 (1992).





# Upgrades to VB Diagnostic Increase Throughput

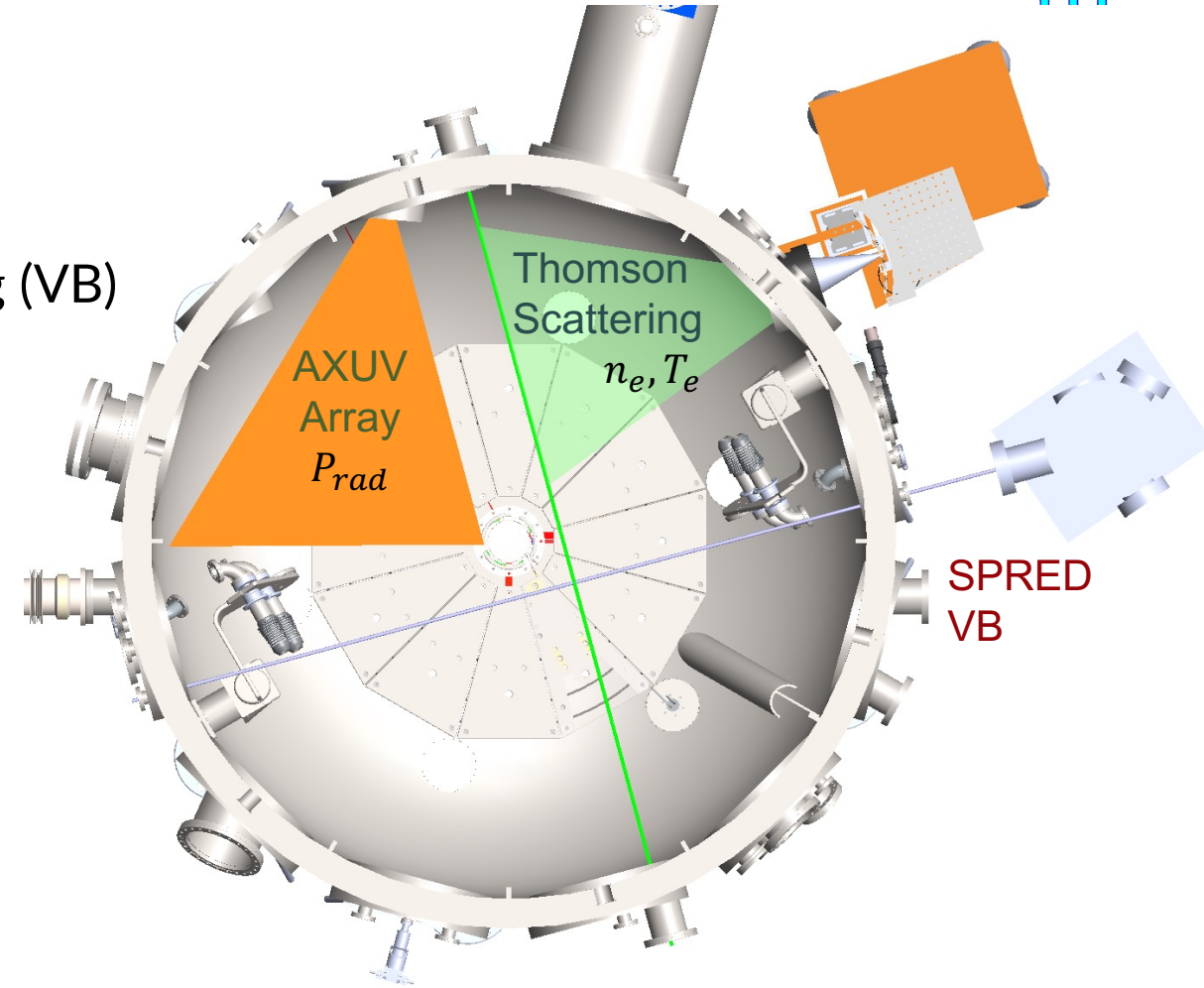
- Low radiance is expected for PEGASUS-III
  - $n_e \sim 1 \times 10^{19} \text{ m}^{-3}$ ,  $T_e \sim 100 \text{ eV}$
  - $B_{brems} = \int \epsilon ds \sim 1 \times 10^{10} \frac{\gamma}{s} \frac{1}{\text{cm}^2} \frac{1}{\text{nm}}$
- Throughput to be increased by  $\sim \times 10$ 
  - Ten 1 mm f/2 fibers collect light
  - Introduced fast shutter ( $\sim 2 \text{ ms}$ )
  - Vertical binning of the full CCD
- Expected Counts (DN)  $\sim 20$ 
  - $U = 1.4 \times 10^{-2} \text{ cm}^2 \text{ sr}$  (SpectraPro 275)
  - $QE = 70\%$ ,  $G = 0.125 \text{ DN/photons}$
  - $\Delta\lambda \approx 1 \text{ nm}$
  - $DN = B_{brems} \times U \times QE \times G \times \Delta t \times \Delta\lambda$





# Impurity Studies will Utilize Multiple Diagnostics

- Species Identification with SPRED
- $Z_{eff}$  measurements with Visual Bremsstrahlung (VB)
  - Needs  $n_e$  and  $T_e$  from Thomson Scattering
- AXUV radiometry for  $P_{rad}$
- CHERS is under development\*
  - Can directly measure impurity densities
- Impurity transport modeling with STRAHL



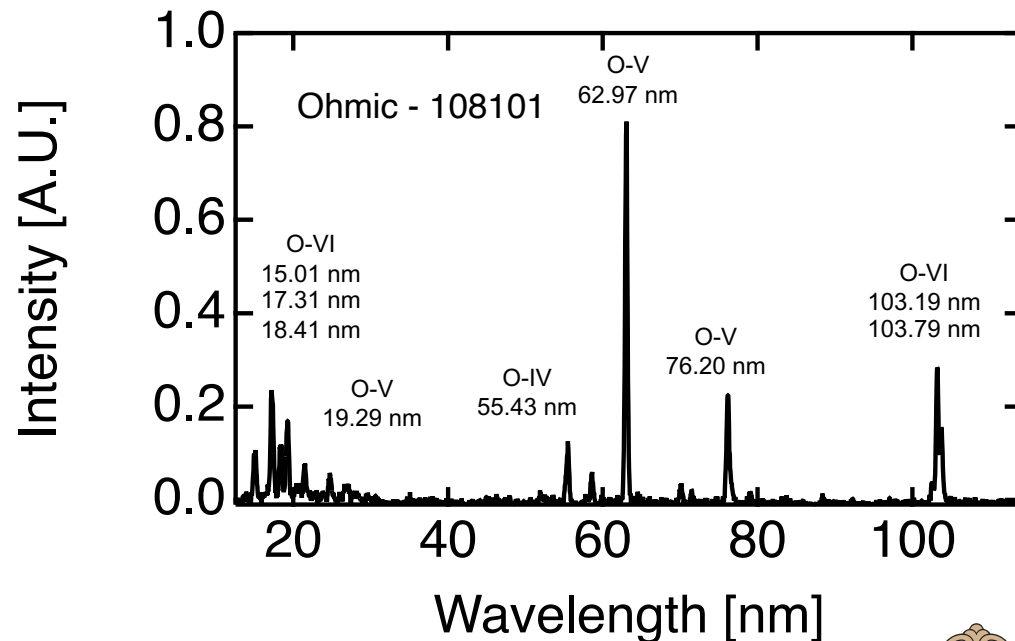


# VUV Spectra Suggest Increased Impurity Influx During LHI



## Ohmic Discharge

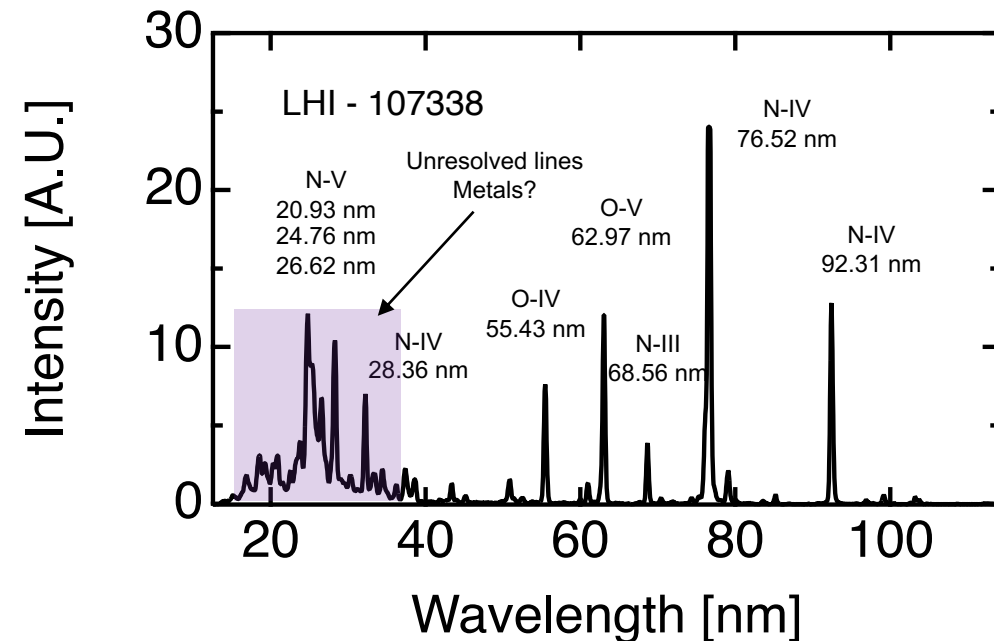
- Oxygen dominated
- Low intensity (100s counts)



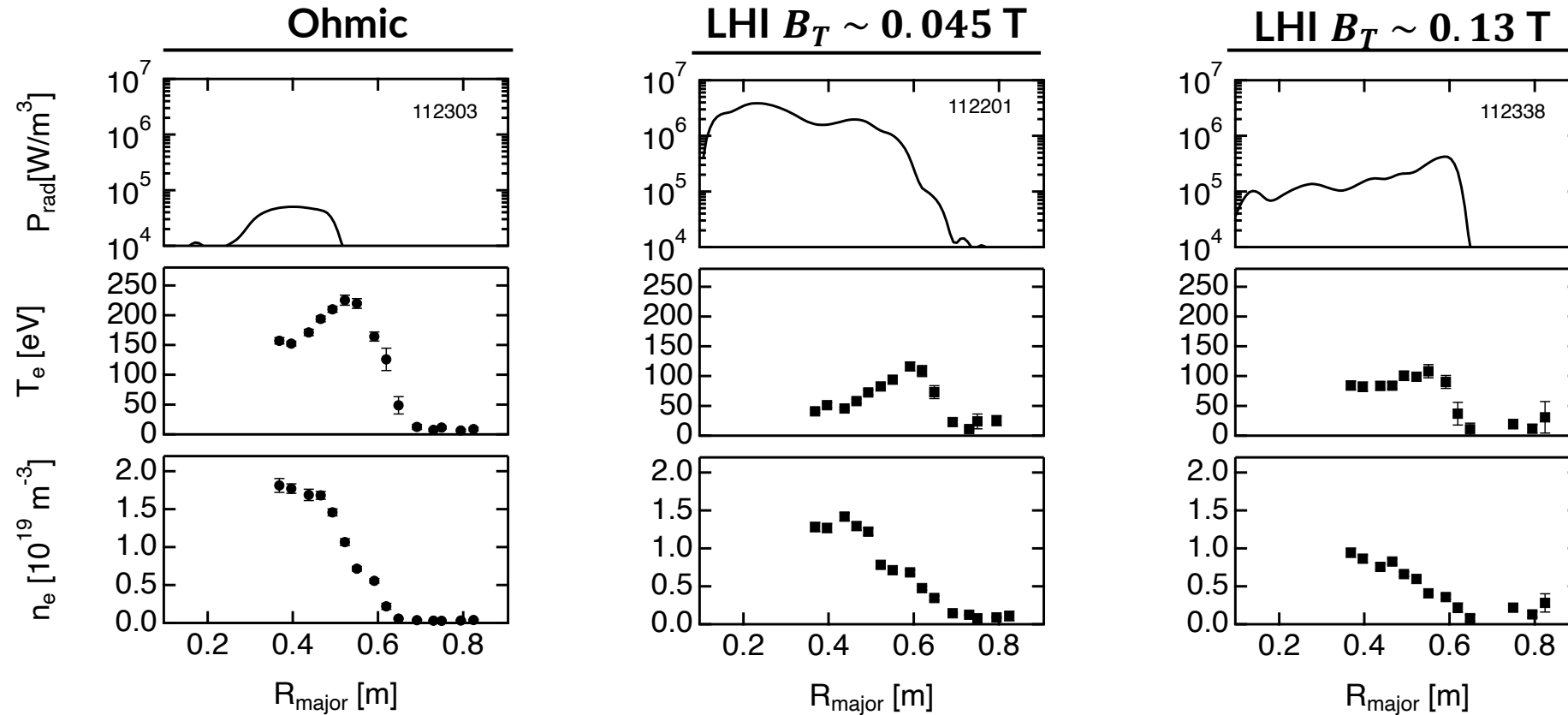
## LHI Discharge

- Nitrogen and oxygen Identified
  - Possible sources are plasma material interaction
- Intensity is higher than Ohmic
  - At similar  $n_e$  and  $T_e$ , this suggest higher  $n_{imp}$

$$\epsilon \propto n_e n_{imp} \langle \sigma(T_e) v \rangle$$

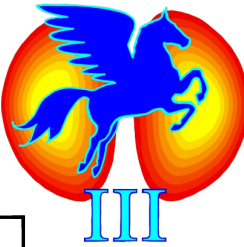


# Clear Differences in $P_{rad}$ are Observed Between Ohmic and LHI and Between Different $B_T$ Levels



- AXUV diode sensitivity drops for photons with energies  $< 50$  eV
  - Currently working on correction factor to account for change in diode response



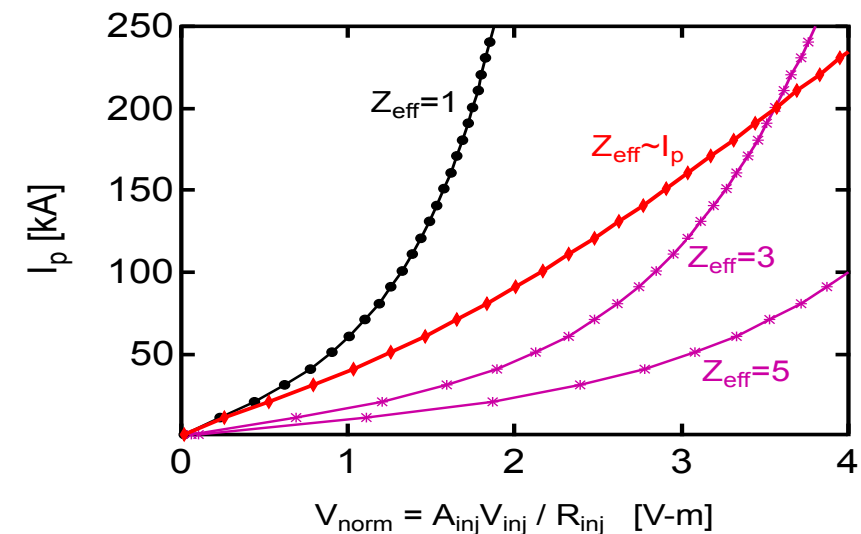
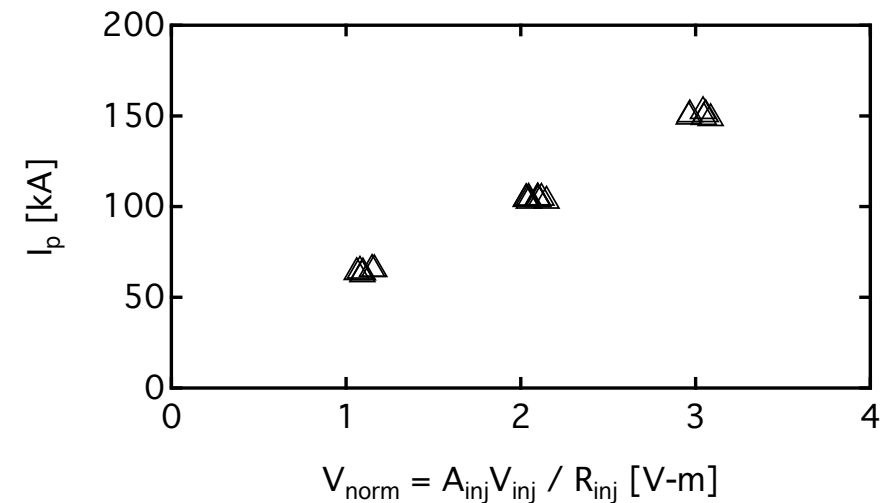


# Observed $I_p$ Trends Motivate Measurements of $Z_{eff}$

- $I_p \propto V_{LHI}$ 
  - Implies constant  $\langle \eta \rangle$
  - Motivates efforts to determine  $Z_{eff}$
- Bremsstrahlung continuum can be used to measure  $Z_{eff}$

$$\frac{d\epsilon}{d\lambda} = 7.632 \times 10^{-15} \frac{n_e^2 g_{eff} Z_{eff}}{T_e^{1/2} \lambda} e^{-\frac{hc}{\lambda T_e}} \left[ \frac{\gamma}{s} \frac{1}{\text{cm}^3} \frac{1}{\text{nm}} \right]$$

- Other sources of emission may complicate measurement:
  - Line radiation
  - Electron-neutral bremsstrahlung
  - Molecular hydrogen emission





# Impurity Transport Modeling



# Transport Code STRAHL is Used for Impurity Studies

- STRAHL<sup>1</sup> is an impurity transport code that solves the continuity equation
- Code outputs: impurity densities and emission
- 1-D cylindrical equation obtained if particle flux is averaged over a flux surface

$$\frac{\partial n_{I,Z}}{\partial t} = -\nabla \cdot \vec{\Gamma}_{I,Z} + Q_{I,Z} \quad \longrightarrow \quad \frac{\partial n_{I,Z}}{\partial t} = -\frac{1}{r} \frac{\partial}{\partial r} r \left( D \frac{\partial n_{I,Z}}{\partial r} - v n_{I,Z} \right) + Q_{I,Z}$$

- Impurity flux separated into diffusive and convective term
  - Diffusion is proportional to  $\nabla n_{I,Z}$
  - Convection is proportional to  $n_{I,Z}$
$$\Gamma_{I,Z} = D \nabla n_{I,Z} + v n_{I,Z}$$

- Radial label is related to the flux surface volume

$$r = \sqrt{\frac{V}{2\pi^2 R_0}}$$

- Sources/sinks couple neighboring states

$$Q_{I,Z} = -(n_e S_{I,Z} + n_e \alpha_{I,Z} + n_H \alpha_{I,Z}^{cx}) n_{I,Z} \\ + n_e S_{I,Z-1} n_{I,Z-1} \\ + (n_e \alpha_{I,Z+1} + n_H \alpha_{I,Z+1}^{cx}) n_{I,Z+1}$$

- Ionization ( $S_{I,Z}$ ), recombination ( $\alpha_{I,Z}$ ) and charge exchange ( $\alpha_{I,Z}^{cx}$ ) rates obtained from ADAS<sup>2</sup>

<sup>1</sup> R. Dux, "STRAHL User Manual," IPP Report 10/30, 2006.

<sup>2</sup> H.P. Summers and M.G. O'Mullane, in *AIP Conference Proceedings* (2000), pp. 304–312.

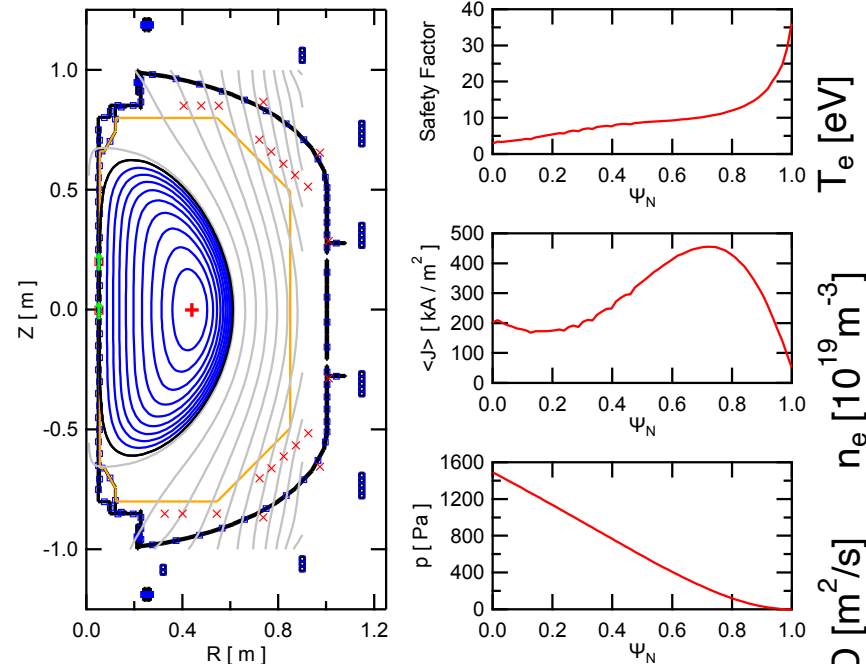


# Initial Analysis With STRAHL for an LHI Discharge



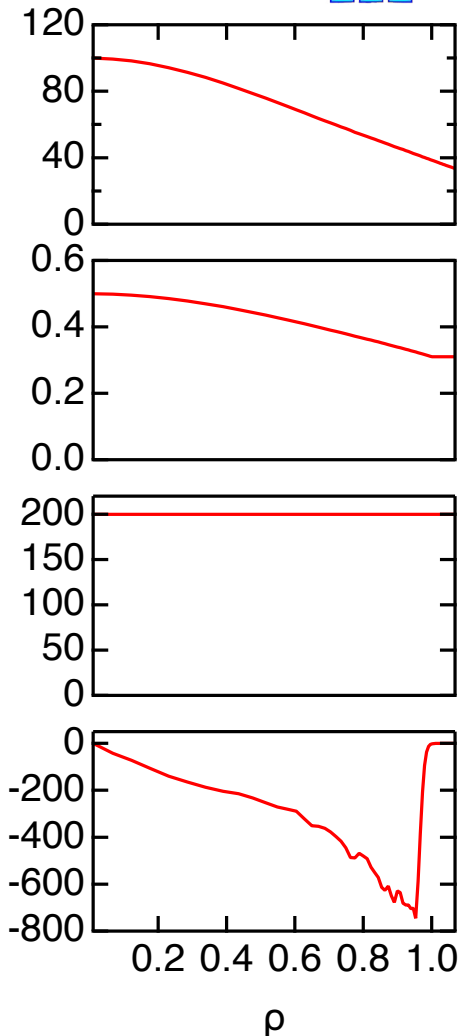
## • Inputs to the code

- Magnetic geometry from equilibrium reconstruction
- Peaked background pressure profile
  - $T_{e0} = 100$  eV
  - $n_{e0} = 0.5 \times 10^{19} \text{ m}^{-3}$
- Transport coefficients
  - $D \sim \frac{a^2}{\tau_E} \sim \frac{a^2}{\tau_p} \sim 200 \text{ m}^2/\text{s}$
  - Neo-Alcator scaling predicts  $\tau_E \sim 0.5 \text{ ms}$
  - $v = D \frac{1}{n_e} \frac{dn_e}{dr}$  if steady-state  $n_{imp}$  is assumed
- Source rate chosen such that  $\frac{n_{imp}}{n_e} \sim 1.5\%$ 
  - Localized at the plasma edge  $\rho > 1$

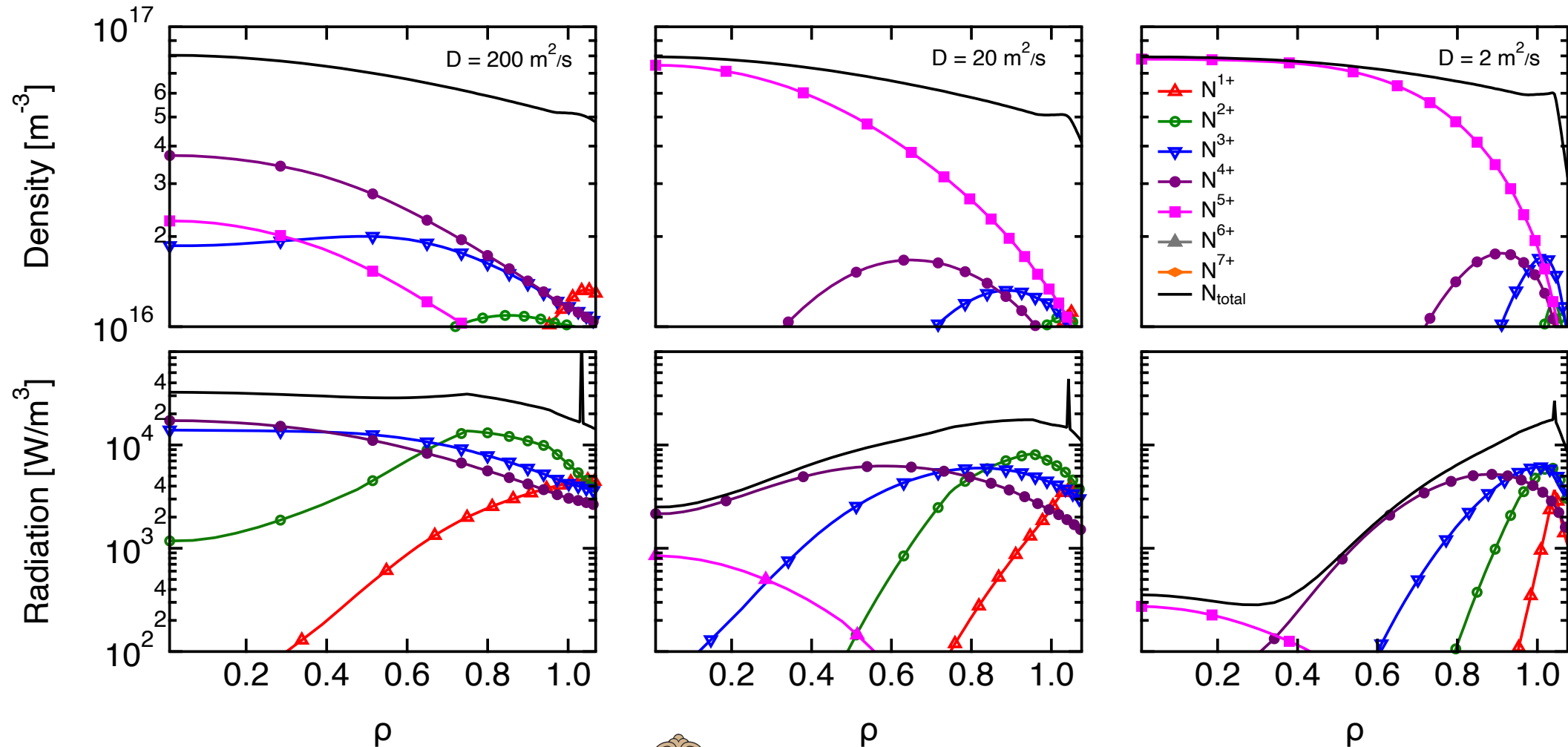


Equilibrium Parameters  
Shot 107381, 27.00 ms

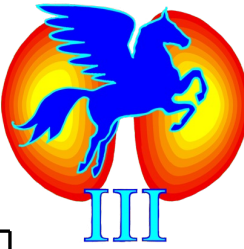
$I_p$	163 kA	$R_0$	0.333 m
$\beta_t$	0.059	$a$	0.278 m
$I_i$	0.27	$A$	1.20
$\beta_p$	0.39	$\kappa$	2.2
$W$	1579 J	$\delta$	0.51
$B_{T0}$	0.181 T	$q_{95}$	21.9



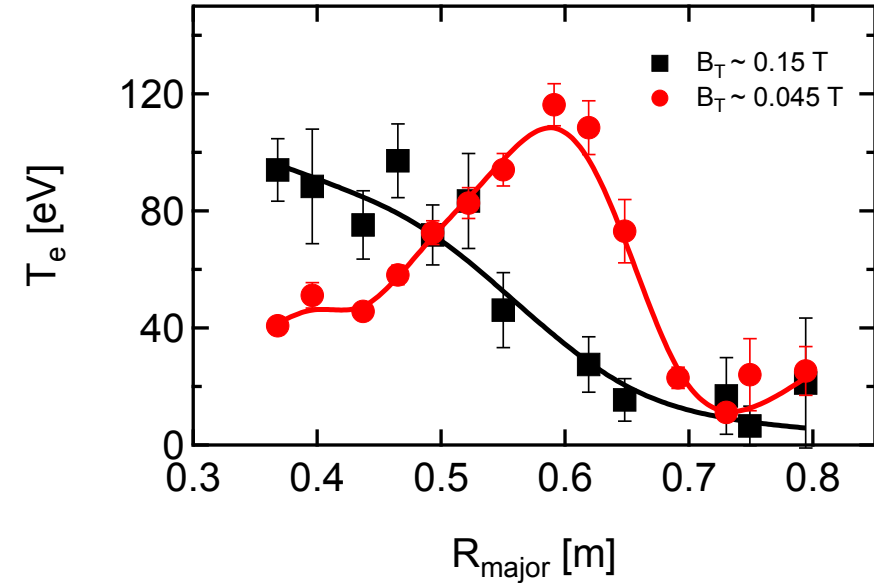
# Reduced Impurity Transport Affects Charge-State Balance and Radiation Profile



# Strong Impurity Transport May Explain Observed $T_e$ Profiles



- LHI hollow current profiles  $\rightarrow$  low core Ohmic heating<sup>1</sup>
  - $\eta J_0^2 \sim 10 \text{ kW/m}^3$
- Strong transport leads to high core radiation
  - Low, highly radiative charge states can exist in the core
  - Flat radiation profile
  - $P_{rad,0} > \eta J_0^2$
- Reduced impurity transport  $\rightarrow$  hollow  $P_{rad}(R)$ 
  - Low charge states reside only at the edge
- Reduced transport expected at higher  $B_T$
- In all cases  $P_{rad} < P_{in}$



$D$ [m <sup>2</sup> /s]	$P_{rad,0}$ [kW/m <sup>3</sup> ]	$P_{rad,a}$ [kW/m <sup>3</sup> ]	$P_{rad}$ [kW]
200	32.5	18.1	28.5
20	2.5	15.7	12.8
2	0.3	15.9	4.7



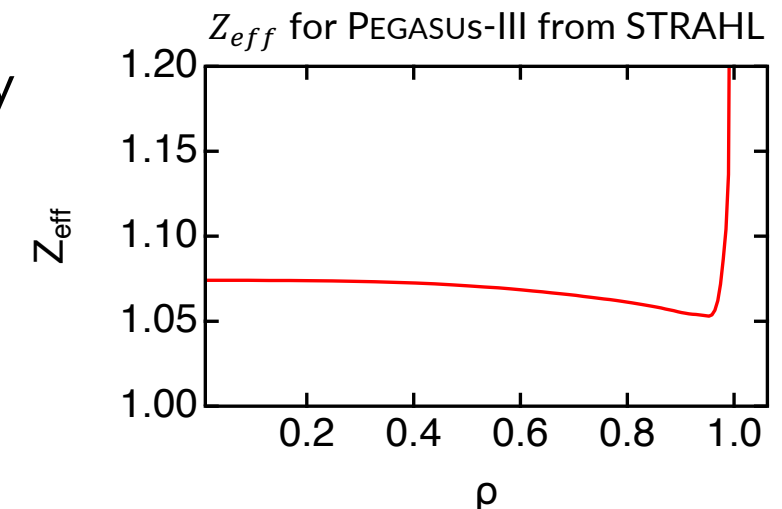
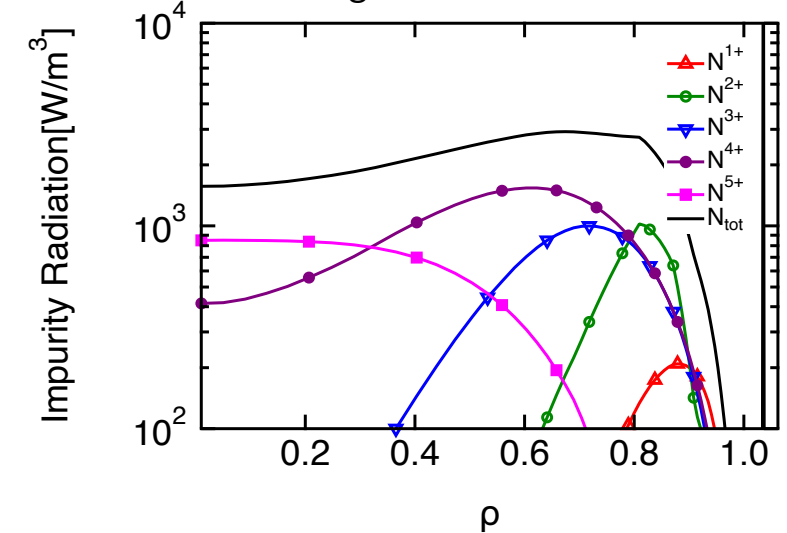
# Impurity Assessment on PEGASUS-III

# LHI Impurity Sourcing, Concentrations and Effects on LHI Performance Will be Explored in PEGASUS-III



- Experiments will characterize impurity sources from LHI
  - Cathode spots from injectors
  - Injector structures
  - Sputtering/ablation of wall materials due to electron beam
  - Combination of SPRED gratings allow to observe impurity lines
- Impurity concentration will be inferred through  $Z_{eff}$ 
  - Simulations with STRAHL predict flat  $Z_{eff}(R)$
  - Line-averaged  $Z_{eff}$  measurements with VB
- A more direct calculation of resistive dissipation and helicity drive
  - Helicity dissipated resistively
  - Needed for reliable  $I_p$  projections

Simulated Nitrogen radiation for PEGASUS-III

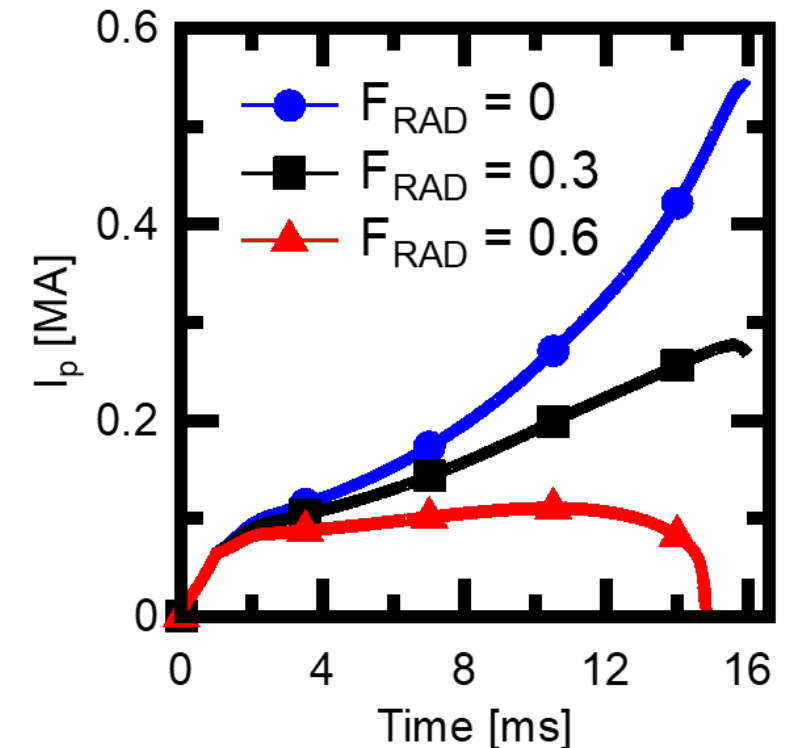


# Experiments will Investigate Impact of Impurity Transport in LHI Startup and Power Balance



- Transport could play an important role in resistive dissipation
  - Possible cooling of  $T_e$  if high core radiation
- Changes in  $B_T$  may induce changes in transport
  - Evidence of improved transport at higher field seen on PEGASUS
  - New PEGASUS-III TF coils permit a wider  $B_T$  scan
- Transport determined from STRAHL and experiments
  - Use measured  $P_{rad}(R)$  and  $Z_{eff}$  as constraint for STRAHL
- Radiation losses important for power balance

Projected  $I_p$  evolution on PEGASUS-III at different fractions of radiated power\*



\*See J. D. Weberski CP11.00049





# Influence of Impurities on H-I Tokamak Startup will be Studied in PEGASUS-III



- Impurity studies are needed for better LHI projections
  - Impurities affect helicity dissipation through changes in resistivity
    - Increase in mean ionic charge and cooling
  - Radiation power losses impact power balance
  - Accurate  $I_p(t)$  projections require a model to scale helicity dissipation
- A suite of diagnostics and tools will be used to do an impurity assessment
  - Species identification with SPRED
    - New high-resolution grating will help to resolve previously unresolved lines
  - VB spectroscopy for  $Z_{eff}$ 
    - Throughput of the diagnostic increased by  $\sim 10\times$
    - New spectral survey planned to find region free of line emission
  - AXUV radiometry for  $P_{rad}$ 
    - New 32-channel designed, calibrated and ready for operations
  - Impurity Transport modeling with STRAHL

